Ignition from High Heat Flux for Flat versus Complex Geometry

Brown A.L.[1,*], Engerer J.D.[1], Ricks A.J.[2], Christian J.M.[3]

[1] *Sandia National Labs, Fire Sci. and Tech. Dept., Albuquerque, NM, USA*
[2] *Sandia National Labs, Tech. Anal. Dept., Albuquerque, NM, USA*
[3] *Sandia National Labs, Conc. Solar Tech. Dept., Albuquerque, NM, USA*
**Corresponding author's email: albrown@sandia.gov*

ABSTRACT

Ignition of solid materials from radiative heat flux has been well studied, as it relates to common fire instantiation and propagation. Conventional testing involves a small (~10 cm) flat sample in a test apparatus such as a cone calorimeter exposed to fluxes in the range of 25-100 kW/m^2. Higher heat flux ignition has been less-well studied, and the majority of scientific data come from similarly scaled experiments mostly on flat surfaces. High heat flux ignition is less well studied because it has a more limited application space given that fewer fire scenarios involve high (> 200 kW/m^2) fluxes. We have been performing experimental investigations of the behavior of a variety of materials exposed to concentrated solar power with peak flux in excess of 2 MW/m^2. Dozens of materials at a variety of flux conditions with varying scales and configurations have been tested thus far. While we have found good correlation in our new data to historical data and model constructs, some of our data are not well predicted by existing models and correlations. Present results suggest ignition on flat materials is not necessarily a good predictor of other materials and configurations, and that future testing would benefit from an increased emphasis on the geometry of exposed materials.

KEYWORDS: Ignition, heat flux.

INTRODUCTION

Ignition from an incident radiative flux is well characterized for many materials under flux conditions typical of conventional hydrocarbon fires (25-100 kW/m^2). Standards such as ASTM E1740-15 and ASTM E1354 govern this type of testing. We are focused on ignitions and fire behavior from much higher fluxes (100-10,000,000 kW/m^2), which may be obtained from metal fires, propellants, lightning, directed energy, space exploration, etc.

Historical data on ignition from high heat fluxes are not as plentiful. Notable compilations of data in this flux regime include Glasstone and Dolan (1977) [1] and Martin and collaborators [2-3]. Glasstone and Dolan correlated ignition for a variety of materials to the yield and distance from a nuclear weapon, a construct that is not particularly useful in other applications. Martin et al. represented their ignition data in terms of scaled flux and fluence, a more useful construct for extensibility. The Martin datasets are dominated by cellulose paper data and exposure areas of around 10 cm^2, the primary focus of their efforts. They found various behavioral regimes characterized by different parameters. At low fluxes, the sample thickness and imposed energy were most significant. At higher fluxes, the incident energy was the dominant parameter. At even higher fluxes, the imposed energy and the flux magnitude had comparable significance. Different types of ignition were observed (glowing, sustained flaming, transient flaming). Transient flaming was defined by flaming that occurred only as the heat flux was incident on the object. Sustained flaming lasted beyond the exposure.

Proceedings of the Ninth International Seminar on Fire and Explosion Hazards (ISFEH9), pp. 970-979
Edited by Snegirev A., Liu N.A., Tamanini F., Bradley D., Molkov V., and Chaumeix N.
Published by Saint-Petersburg Polytechnic University Press
ISBN: 978-5-7422-6498-9 DOI: 10.18720/spbpu/2/k19-92

We have been adding to the body of work on high-heat flux ignition by testing materials under high flux (> 200 kW/m^2) conditions using concentrated solar energy. Work began with a focus on flat materials with an objective to reach-back to the majority of the historical data [2-3], but has included enough geometric variation to begin to deduce the important role geometry has in the ignition behavior. Our prior reporting of this work illustrates the significant role of scale in the fire behavior [4], a new approach to the ignition and damage threshold modelling [5], and the effect of wind and gas phase radiation attenuation on the fire response of materials [6].

Evaluations of the recent data suggest an additional significant feature of the materials that appears to affect the outcome of the event. The shape of the samples appears to affect the resultant ignition behavior. The effect of shape is not systematically studied in any of the historical datasets, and consequently is ignored in prior models and inferences derived therefrom. More complex shapes may tend to more easily ignite and sustain ignition. This paper examines the evidence for this statement in the context of the recent concentrated solar ignition tests. The purpose and value of this paper is in the identification of the important role that shape has on the propensity for sustained ignition from high heat flux events. The objective is to help motivate an increased exploration of the shape as an important factor leading to high heat flux ignition to better characterize a broader range of material response.

METHODS

The National Solar Thermal Test Facility at Sandia National Labs in Albuquerque has two main facilities that concentrate solar energy. One is the Solar Tower, that uses a heliostat field (an array of large mirrors with fine motor control that actively track the sun to maintain a relatively constant target location for the rays) to achieve a concentration factor greater than 2000 suns (1 sun is approximately 1 kW/m^2), and a power of 6 MW at length scales of 0.3-1 m. The other is the smaller Solar Furnace that uses a single heliostat and a parabolic dish for smaller length scale testing (5-7 cm). Several hundred high flux ignition tests have been conducted at these facilities including varying material types, thicknesses and shapes, while also varying flux, fluence, length-scale, wind, and ambient temperature.

Tests were conducted in test phases. A Solar Furnace test phase involved approximately 50 test shots, while the solar tower test phase involved about 30 shots. The test matrix for each test was determined by a panel of researchers. Materials were selected from a list of relevant materials. Test and environment conditions were controlled as well as could reasonably be done for the facilities available. Test objectives were manifold, so the test programs were not apparently targeted in their approach to specific objectives. Rather, a wide variety of materials and test conditions were employed with the outcome of the tests being the identification of prospective subsequent tests to explore interesting observations from prior test phases. The three main programmatic objectives were:

1. To produce quality datasets with sufficient repeatability to employ for validating 3D computational models of fire and related phenomena.
2. To explore environmental factors with the intent of reach-back to historical datasets to understand material dynamics under various conditions.
3. To explore practical or unique ignitions that are under-represented in the body of historical testing.

Tests were split roughly evenly between the above three objective areas. The reason for testing in phases while incorporating multiple objectives is because of the uncertainties in funding cycles and the desire to have broad impact rather than narrowly focused program results. A negative

consequence of this method is that it may take multiple test phases to achieve sufficient data to quantitatively resolve phenomenology from the tests. An advantage of the method is that a targeted assessment is made after each phase of testing, and the subsequent plans are formulated after gaining insight from the results from prior phases.

Table 1 shows some details of the sample tested. Flat samples were 23×11.5 cm at the solar furnace, and approximately 90×120 cm at the solar tower. L-shaped samples consisted of two chairs, photographs of which are shown in Fig. 1. A polypropylene patio chair and a wood/foam/fabric office chair were used. Chairs were oriented differently during the tests to optimize exposure to the incident flux. The polypropylene chairs were upright with the back of the seat back exposed to the flux, and the fabric chairs were on their side with the front of the seat back in direct exposure.

Table 1. Details regarding the reported Solar Tower (ST) and Solar Furnace (SF) experiments

Material	Geometry	Thickness (mm)	ST	SF
Cellulose	Flat	1.2-5.0		X
Paper	Flat	0.11-0.25	X	X
Fabric	Flat/L	0.7-0.9	X	X
Biomass	Irregular/Flat	Variable	X	X
Polyethylene	Circular/Flat	≈ 3 mm	X	X
Polystyrene (PS)	Flat	0.5-3.2	X	X
Synthetic Rubber	Circular/Flat	Variable	X	X
Polymethyl-methacrylate (PMMA)	Flat	3.2-11.3	X	X
Polypropylene	L/Flat	Variable < 4	X	X
Vinyl	Flat	1.1		X

Fig. 1. Pre-test photographs of the polypropylene (left) and wood/foam/fabric chairs (right).

INSTRUMENTATION

A variety of instrumentation was deployed for the tests, the details of which may be found in the test series documentation. For this paper, highlights of the instrumentation are outlined only. Details on the instrumentation are available in the corresponding test phase documentation [3-6]. Each test included the following:

1. Flux measurements to confirm the imposed thermal environment, and characterization of the day, time, and configuration of the flux source

2. Multiple angle fiducially accurate video imagery from standard, high-speed, and filtered optical cameras
3. Atmospheric data from a weather station to confirm the ambient conditions
4. Pre- and post-test photography
5. A temporal fiducial to allow post-test synchronization of instrumentation results from various sources
6. Controls output containing data on the temporal sequence for each test

Tests mostly included:

7. Pre- and post-test weight of samples

Some tests included:

8. Strategically mounted thermocouples for temperature measurements
9. IR camera imagery for thermal response
10. Witness strings as local air flow indicators
11. Post-test 3D scanning for digital re-construction of the thermal crater

Ignition and burn times are key to the analysis presented in this paper. These were deduced through post-test analysis of the video imagery. Ignition was often discernable through the observed flames in the video output. In some tests, the pyrolysis gases obscured direct views of the ignition. The ignition event usually included a rapid increase in the motion of the pyrolysis gases, in which case the flames were not directly observed but inferred based on the motion of the opaque gases and the presence of flaming later in the video.

Characterization of Environment

Tests were conducted within a few hours of solar noon on clear (cloudless) days. The environment was characterized using pre- and post-test analysis of heat flux instrumentation to verify the test conditions. Because of the response time of the test facility hardware, the imposed flux was a ramp to a constant hold, and a ramp back down to ambient.

Fluence (defined as flux integrated with time) magnitude was a target condition, which explains the regularity of intervals in some of the fluence data. Fluence targets were usually round numbers, however post-analysis sometimes adjusted these away from the target values. For this paper, exposures are simplified to a fluence condition. Solar Furnace fluence was applied over a roughly 4-6 cm diameter spot [7], Solar Tower exposures varied spatially, but spanned the samples. Peak flux and fluence was centered on each sample.

Tests were conducted at different times of the year in an outdoor environment. Ambient temperatures for two Solar Furnace test series conducted in July/August were 20-35ºC. The second Solar Furnace phase was conducted in February/March, and mid-day ambient temperatures were between 5-25ºC. The Solar Tower tests were conducted from August-November, and ambient temperatures varied between 10-30ºC. Post-processing of the data has not suggested a significant effect of the initial ambient temperature on any resultant parameters over the range of variation.

RESULTS AND DISCUSSION

We grouped materials in a few categories for this analysis. The first main grouping is by material type. Cellulosic materials (plant matter, paper, wood, fabrics, etc.) are grouped, as cellulose constitutes a significant fraction of these materials. Synthetic polymers are also grouped. The second grouping consists of the shape of the test objects. Flat objects are primarily surfaces exposed to the flux, and represent the traditional way of assessing ignition at high heat flux. A few of the

samples consisted of significant L-shapes, and these are termed L-shaped materials. Some materials were round (tires and trash cans). They differ from the flat materials because there were no significant flat surfaces, and the curves were the dominant shape of the exposed surfaces. These are termed circular. Irregular shapes are generally biomass materials that are characterized by high surface area compared to the volume.

The test series involved more tests than are exhibited here. Tests omitted include ones that defied characterization by the shape parameters (flat, circular, L and irregular), those that did not fit the material type categorization, as well as those that did not achieve flaming ignition.

Combining the duration of burn results with the fluence imposed on the samples, a picture emerges suggesting a significant role that shape plays in the duration of burn. For convenience in plotting, burn durations greater than 1000 seconds have been truncated to 1000, and durations below 1 second have been increased to 1. While this is not a hard rule, it turns out that tests that involved transient flaming all are below 10 s burn time, and the sustained flaming tests all fall at or above 10 seconds. Figure 2 shows a plot of cellulosic materials on the fluence/burn duration plot. There is a very clear stratification between the data by shape. The few L-shaped tests show generally higher burn durations than other tests. The irregular shaped objects tend to have higher burn durations. The flat materials exhibit generally lower burn durations. There were no 'circular' samples for the cellulosic materials.

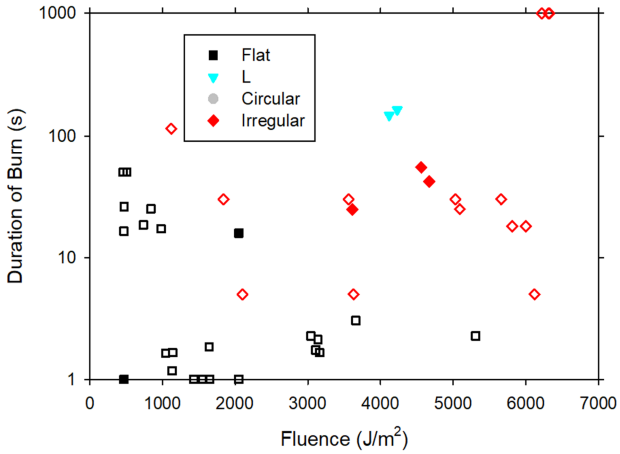

Fig. 2. Duration of burn versus fluence for cellulosic samples. Solar Tower experiments are differentiated from Solar Furnace tests, having closed symbols instead of open.

Because the tests were not systematically varied specifically for this parameterization, there is a need to interpret the meaning of these results in the context of a more representative evaluation including the other variabilities. The flat materials generally did not result in sustained burning. The general exception to this is flat materials that were sufficiently thin that the imposed radiant energy pyrolyzed the sample completely through. Figure 3 illustrates some sustained ignition of thin materials fitting the just described behavior. The fire was initially (post-exposure) localized to edges on the sample, typically a circular ring at the center of the sample. Thicker samples pyrolyzed, but would not sustain flaming if they ignited. The flat materials that sustained flaming were all sufficiently thin to burn in this manner. It is not a particular surprise to see the irregular shaped materials generally exhibiting longer burn times. When burning solid materials, the surface area to volume is widely recognized to be a very significant parameter. The three irregular samples that fall below 10 s burn duration were a mix of green and dry needles. The green needles alone did not ignite, and the dry needles alone generally burned profusely. The large-scale (Solar Tower) and

some of the small-scale tests were green plant materials. The trees at the Solar Tower were cut within 30 minutes of their exposure, and were well watered. Even with the high moisture content of a live tree that normally is expected to inhibit flaming, the irregular materials appear to result in much greater burn times than was typical of the flat biomass samples. This suggests a more significant effect of shape as compared to moisture in these tests.

Fig. 3. Two thin rectangular Solar Furnace samples exhibiting sustained flaming at/within the rim of the hole. The left figure is a walnut veneer at 3.5 seconds, and the right figure is black polystyrene at 3.5 seconds. Figures were enhanced with adjustments to brightness and contrast.

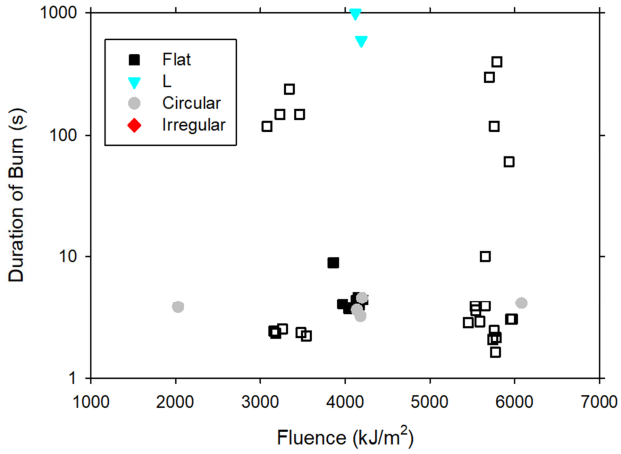

Fig. 4. Duration of burn versus fluence for synthetic polymer samples. Solar Tower experiments are differentiated from Solar Furnace tests, having closed symbols instead of open.

A similar plot of burn duration versus fluence for the synthetic polymer samples is shown in Fig. 4. These data lacked samples that could be considered 'irregular', however included a number of samples that could be considered circular. The response of flat synthetic polymer samples was observed to be similar to that of cellulosics in that the tests tended to produce transient flaming results unless the samples were thin and holes were formed in the material at the center of the exposure. The L-shaped chairs exhibited the longest flaming, and this was surprising. The same polypropylene chair seats had been cut and tested at the Solar Furnace as flat panels at higher fluxes. They did not ignite, even with a higher flux/fluence condition. The differing ignition/non-

ignition behavior was not particularly surprising, as PMMA flat panels behaved similarly with scale changes. What was surprising was that the flaming was sustained for a very long time without the immediate burn-through that seemed to be the contributing factor for flat materials to exhibit sustained burning. There were multiple L-shapes on the polypropylene chairs. The seat/back formed L's. But the legs and seat also had smaller L-shaped structural members. It was at these that flaming was sustained. The chair back melted and sloughed during the exposure and was not able to maintain the L-shape through to the end of the exposure. The seat was made of thicker and more rigid material, and was oriented less orthogonal to the incident flux. The seat and legs remained mostly rigid during the test (one leg burned through long after the exposure).

The circular materials were only tested at the Solar Tower, and resulted in transient flaming, consistent with flat surfaces. There was postulation ahead of the testing that the trash can with a circular cavity might augment ignition and burn prospects due to the ability of the material to retain more energy by radiating within the cavity. The tests did not suggest that this was a significant effect. The circular materials generally agreed with the flat materials in terms of burn duration.

Because the burn duration relates to the size of the samples in the sense that full burn-out limits the potential for longer burn durations, there is a desire to filter the data to differentiate on this effect. It is also desirable to differentiate the comparatively thick samples that classically are only ignited in the transient mode. The normalization of the fluence is done by Martin et al. by the heat capacity of the material. The resultant parameter is not fully non-dimensionalized, as the scaled parameter retains units of temperature. Martin et al. found for cellulose that sustained flaming was generally attained when the scaled fluence was greater than 1000 K. Below 1000 K there was either no flaming or transient flaming depending on the magnitude of the scaled flux. The relation for the scaled fluence is:

$$Scaled\ Fluence = \frac{\alpha q''}{\rho C_P L} \tag{1}$$

Here α is the absorptivity, q'' is the imposed fluence (J/m^2), ρ is the bulk material density (kg/m^3), Cp is the specific heat of the solid (J/(kg·K), and L is the characteristic length (m), which is the primary thickness of the samples. Thermal properties were estimated from measurements (typically density, absorptivity, fluence, and thickness) and common literature sources (specific heat and select others), and are expected to be accurate to within at least 10%. This accuracy is believed adequate for the purposes of this analysis.

We re-cast the burn duration data in terms of the scaled fluence in Figs. 5 and 6, providing a comparison back to the historical sustained flaming threshold. The cellulosic materials in Fig. 5 show a reasonably consistent trend with the expected transition based on the data of Martin et al. to sustained flaming above 1000 K (the green line). Some transient flaming is observed for materials with higher scaled fluence than 1000 K. These flat materials were mostly the wood veneers. The irregular materials that fit this category included the mix of dry and green needles. Transient flaming data below 100 K scaled fluence included a stack of 50 copy paper pages. These ignited in an expected regime because the scaled flux was relatively high (even though scaled fluence was relatively low; the construct of Martin et al. allows for this). Some sustained flaming was observed for samples with lower scaled fluence than 1000 K. This included most notably the solar tower fabric test. The L-shaped chairs had noticeably high burn duration compared to other samples at the same scaled flux, but were in a regime where ignition was not unexpected.

Even though Martin et al. imply that scaled fluence ignition thresholds for different materials might be different, we have generally found the cellulose scaled ignition data to roughly coincide with the data from the common polymer samples we have been testing thus far. The synthetic polymer data in Fig. 6 might also be expected to transition between transient and sustained flaming at about 1000 K on the scaled fluence axis. The L shaped polypropylene chairs are a notable exception. They

are moderately below the threshold, yet exhibited the greatest burn duration. This is added evidence for the significance of the L-shape to the ignition and burn duration. A cluster of flat materials had scaled fluence around 2000 K but did not sustain ignition. These are solid vinyl and thicker polystyrene samples. The circular samples that did not sustain ignition all fall below 1000 K, suggesting that they were not necessarily expected to. All flat samples that sustained ignition had scaled fluence above 1000 K. These were mostly burn-through scenarios involving comparatively thin materials.

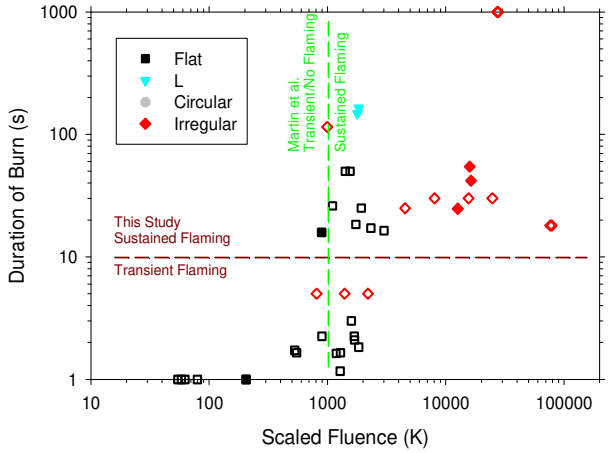

Fig. 5. Duration of burn versus scaled fluence for cellulosic samples. Solar Tower experiments are differentiated from Solar Furnace tests, having closed symbols instead of open.

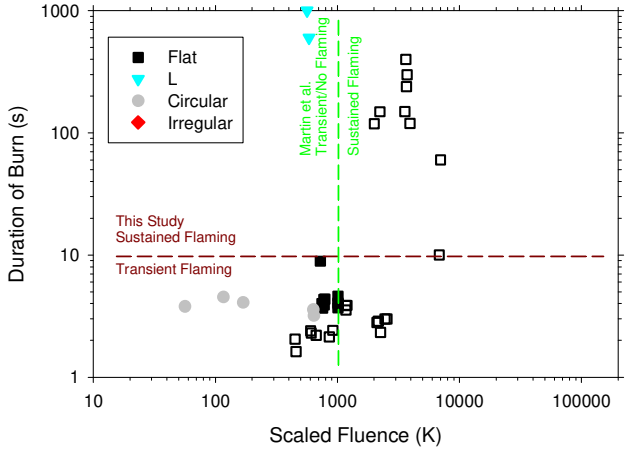

Fig. 6. Duration of burn versus fluence for synthetic polymer samples. Solar Tower experiments are differentiated from Solar Furnace tests, having closed symbols instead of open.

GENERAL DISCUSSION

The results presented herein point to a significant effect of the shape parameter on the burn duration and on the ignition of a variety of materials. The fact that what we have called irregular shaped materials are more prone to longer burn durations is not a particularly surprising or novel conclusion. The basis for this expectation is in conventional fire starting where kindling is often used to initiate larger fires. The surface area compared to the volume is augmented, reducing the thermal sink and augmenting the fraction of energy that results in pyrolysis. One would assume the

same behavior and sensitivity might be applicable to high flux conditions as well. The more significant finding is that the chairs that have been characterized as L-shaped are significantly more prone to ignition and sustained burning. The mechanism differentiating L-shaped and flat materials is likely quite different than that between the irregular (high surface area/porous) and flat materials. From a surface area to volume ratio perspective, the L-shaped materials are much more closely related to the flat materials than the irregular materials. L-shaped materials may have two different features that contribute to augmenting the propensity for fire. First, they have the ability of the surfaces to emit or reflect radiation from one to the other, a feature not available to flat surfaces. Second, they create a different flow pattern for the product gases and will interact differently with ambient winds.

Prior to testing these materials, the radiation (first) mechanism was anticipated to be the dominant mechanism that might augment the prospects of burning and ignition. Imposed radiative flux from the concentrated solar panels at these high flux conditions is expected to dwarf any reasonably expected convective heat flux. Post-test, there is reason to attribute greater relative significance to the convective (second) mechanism. Fig. 7 shows images from two chair fire tests. The polypropylene chair illustrated had sustained burning on one of the two symmetrically similar chair legs. Because the radiation flux was relatively symmetric as well, we conjecture that the wind direction was the contributing factor to the continuing burn. The fabric chairs exhibited significant vortical motion in the volume between the seat and seat back. This is best observed in the video results, but the image showing the narrow elongated plume from the chair fire helps illustrate presence of significant vortical flow originating at the fire. The fact that circular geometries with cavities did not sustain ignition also lends to the argument, but the cavity also has the effect of limiting oxygen while the L-shape provides better exhaust pathways for product gases.

Fig. 7. Post-exposure flaming of the polypropylene chair (left) and the fabric chair (right).

There was a noticeable edge effect for flat samples when they experienced burn-through that appears to relate significantly to the sustainability of the fire. Because high flux ignitions involve large energy input, the majority of the historical tests were either similar to the Solar Furnace tests where the samples were much larger than the exposure, or had a mask that eliminated edge effects. This may not be representative of many fire scenarios of interest, in which case there may be reason in the future to examine offset ignitions on samples that contain pre-existing edges in the exposure. On larger-scaled tests, the flames often would originate or be obviously influenced by the sample edges.

Upon evaluating the geometry based ignition performance from these tests, it is recommended that subsequent tests increase the formal study of geometry related parameters. Additional L-shaped tests in particular would be insightful including simplified geometries, scale, wind, and material

variations. Flat panel testing is still useful for reach-back to historical tests, validation scenarios, and semi-infinite geometry scenarios, but may significantly under-represent the ignition and burning potential of more complex geometries. Including pre-existing exposed edges might also help better characterize ignition for a broader range of materials.

CONCLUSIONS

Major findings of this study of ignition from high incident heat fluxes include:

- Sustained ignition appears to be augmented for L-shaped and irregular geometries. Two different chairs exhibited long-term sustained burning in the solar tower tests with long-term flames localized to the internal cavity regions and edges. Irregular shapes like plant material (needles, trees, shrubs, grasses) also exhibited prolonged sustained burning.
- Circular geometries (tires and plastic trash cans) were not as prone to sustained ignition as irregular and L-shaped geometries.
- Flat geometries are more heavily tested historically, but may be poorly representative of more practical (complex) geometries with respect to sustained ignition.
- Flat geometries tend not to exhibit sustained ignition unless they develop (via burn-through) or include exposed irradiated edges.

We consequently recommend increasing the experimental focus on non-planar samples and samples with edges in subsequent testing to better capture the ignitability of a broader range of materials and configurations.

ACKNOWLEDGEMENTS

Sandia National Laboratories is a multimission laboratory managed and operated by National Technology and Engineering Solutions of Sandia, LLC., a wholly owned subsidiary of Honeywell International, Inc., for the U.S. Department of Energy's National Nuclear Security Administration under contract DE-NA-0003525.

REFERENCES

[1] S. Glasstone, P.J. Dolan, The effects of nuclear weapons, Department of Defense, Washington DC, 1977.

[2] S.B. Martin, Fire setting by nuclear explosion: A revisit and use in nonnuclear applications. J. Fire Prot. Eng. 14 (2004) 283-297.

[3] S. Martin, Diffusion-controlled ignition of cellulosic materials by intense radiant energy, Proc. Combust. Inst. 10 (1965) 877-896.

[4] A.L. Brown, J.D. Engerer, A.J. Ricks, J.M. Christian, Scale Dependence of Material Response at Extreme Incident Radiative Heat Flux, The 2018 ASME/AIAA Joint Thermophysics and Heat Transfer Conference, Atlanta, Georgia, June 25-29, 2018.

[5] J.D. Engerer, A.L. Brown, J.M. Christian, Ignition and Damage Thresholds of Materials at Extreme Incident Radiative Heat Flux, The 2018 ASME/AIAA Joint Thermophysics and Heat Transfer Conference, Atlanta, Georgia, June 25-29, 2018.

[6] A.J. Ricks, A.L. Brown, J.M. Christian, Flash Ignition Tests at the National Solar Thermal Test Facility, The 2018 ASME/AIAA Joint Thermophysics and Heat Transfer Conference, Atlanta, Georgia, June 25-29, 2018.

[7] C. Ho, S. Khalsa, and N. Siegel, "Analytical methods to evaluate flux distributions from point-focus collectors for solar furnace and dish engine applications," ASME 2010 4th International Conference on Energy Sustainability, American Society of Mechanical Engineers, 2010, pp. 501–509.

Flame retardants

Permanent Flame Retardant Finishing of Textiles by the Photochemical Immobilization of Polyphosphazenes

Opwis K.[1,*], Mayer-Gall T.[1,2], Gutmann J.S.[1,2]

[1] *Deutsches Textilforschungszentrum Nord-West gGmbH, Adlerstr. 1, Krefeld, Germany*
[2] *University Duisburg-Essen, Universitätsstr. 5, D-45117 Essen, Germany*
**Corresponding author's email: opwis@dtnw.de*

ABSTRACT

UV-based grafting processes are appropriate tools to improve the surface properties of textile materials without changing the bulk. Based on our previous investigations on the photochemical immobilization of vinyl phosphonic acid, here, a new photochemical method for a permanent flame retardant finishing of textiles is described using allyl-modified linear polyphosphazenes and derivatives. Exemplarily, we show results on the flame-retardant finishing of cotton and cotton/PET blends with allyl polyphosphazene. We used the terminal allyl group for the photo-induced coupling of allyl polyphosphazene on textile substrates. Using our UV technology 20 to 40 weight percent of the functionalized polyphosphazenes can be fixed covalently to different textile substrates. We observed a slight decrease of the fixed polyphosphazene amount after the first washing cycle indicating the removal of non-bonded molecules. After this initial washing step the add-on is stable. Even after six laundering cycles the modified material withstands various standardized flammability tests. In summary, photochemical treatments allow the permanent surface modification of natural and synthetic fibers by irradiating with UV light in the presence of reactive media. We have successfully demonstrated that these procedures are appropriate for the fixation of flame retardants as well. Polyphosphazene modified textiles show high levels of flame retardant performance even after several textile laundering cycles.

KEYWORDS: Textiles, cotton, polyester, polyphosphazenes, flame retardant finishing.

INTRODUCTION

Textiles made of natural and synthetic polymers such as cotton (CO), polyester (PET) or polyamide (PA) are omnipresent in our day-to-day life. Besides apparel, typical in-door applications are curtains, carpets, bedding or upholstered furniture. Because of their high flammability, these materials represent a potential hazard for goods and life [1]. To achieve flame retardant textiles, the polymers are usually blended or finished with inorganic salts (e.g. nontoxic aluminum or magnesium hydroxide), organohalogens (e.g. chloroparaffins, bromobiphenylether and bromobisphenols) or formaldehyde-based flame retardants [1-4]. Because of their high toxicity the political pressure is growing steadily to replace halogen- and formaldehyde-based flame retardants [5, 6]. Due to the fact that conventional organohalogen-based flame retardants are getting banned more and more, several halogen-free substitutes have been developed, e.g., polyphosphates, organic phosphates or nitrogen compounds [7]. In this context nitrogen and phosphorus-containing chemicals are especially interesting, because of their P-N synergistic effect in flame retardant applications. However, their low stability with regard to washing and mechanical abrasion is limiting their applicability [8, 9]. Furthermore, an increasing amount of organo-phosphorus derivates from flame retardants are found in the environment and even in human tissue. Some of these substances have a potential hormone like effect. Thus, alternative products that combine safety, high flame retardant properties and the possibility to fix them permanently to the textile

Proceedings of the Ninth International Seminar on Fire and Explosion Hazards (ISFEH9), pp. 981-990
Edited by Snegirev A., Liu N.A., Tamanini F., Bradley D., Molkov V., and Chaumeix N.
Published by Saint-Petersburg Polytechnic University Press
ISBN: 978-5-7422-6498-9 DOI: 10.18720/spbpu/2/k19-105

matrix are still desirable. One new approach to achieve flame retardant textiles is the use of layer-by-layer coatings, e.g., the combination of cationic polyelectrolytes such as polyallylamine, chitosan or polyethylenimine with anionic nano-clays, polyphosphates or DNA. Other strategies are based on sol-gel chemistry, carbon nanotubes, polycarboxylic acid, casein coating and photo- or plasma-grafting. More information on textile flame retardants are given in different reviews [10, 11] and books [2, 6-8].

Now, we have identified polyphosphazenes (PPZ) as another promising group of halogen-free flame retardant materials for textile applications. Polyphosphazenes can be divided into different polymer types: linear polyphosphazenes and polymers with cylcophosphazene units (back bone or side chain) [12]. These materials exhibit high limiting oxygen indices [13, 14] and improve the flame retardant properties of polymer blends significantly [14]. Technically, polyphosphazenes are used, e.g. in hydrocarbon insoluble O-rings, biomedical applications, as bio-inert or bio-compatible coatings or in fuel cell membranes. A small number of textile finishings based on polyphosphazenes are already described. Shukal and Arya showed that poly(fluorophosphazene) in combination with organo-bromine compounds improve the flame retardant properties of PET, while it is still unclear if the effect depends on the bromine-containing compounds or the polyphosphazene [15]. Other textile application for polyphosphazenes as finishing agents, textile polymer blending or in a polyurea coating are described in patents. Even fully inorganic polyphosphazenes such as (poly)aminophosphazene, phospham, phosphorus oxynitride and cylcophosphazenes have been used as flame retardants. While these examples demonstrating the general usefulness of polyphosphazenes as flame retardants, no commercial textile PPZ-based finishing is available. The main reasons for this are the lack of polyphosphazenes with appropriate anchor groups for the durable fixation on the fiber surface and suitable process technologies. Because of our experience in the field of photo-initiated reactions for the surface functionalization of textile substrates [16-19], our goal was to develop a flame retardant linear polyphosphazene with sufficient side-chain functionalities, that allow photochemical covalent bonding to typical textile materials, e.g. cotton and cotton/polyester blends.

Generally, polyphosphazenes can be synthesized by different synthetic routes [20]. The most common route is the high temperature ring opening polymerization of the cyclic trimer hexachlorophosphazene in a sealed glass tube developed by Allcock et al. A solvent-based synthesis was developed by the group of Magill [21] that produces polymers with up to 15,000 monomer units. The substitution of the chlorine atoms by, e.g., alkoxy, phenoxy, amino, fluoroalkoxy groups or even mixtures of them results in chemically and thermally stable species [13, 20]. Due to the huge variety of possible side-chain functionalities, the properties of polyphosphazene derivatives can be varied easily, e.g., from water-soluble to highly hydrophobic polymers [22].

EXPERIMENTAL

Textiles and chemicals

Table 1 summarizes the used textiles. Hexachlorotriphosphazene was obtained from Eurolabs Limited (United Kingdom) and allyl alcohol (≥ 99%) from Merck (Germany). Sulfamic acid (≥ 99.3%), calcium sulfate ($CaSO_4 \times 2\ H_2O$, ≥ 98%) and tetrahydrofuran (THF ≥ 99.9%) were obtained from Carl Roth (Germany). 1,2,4-trichlorobenzene (≥ 99%), sodium hydride (55-65%, moistened with oil) and acetylacetone (≥ 99%) were obtained from Sigma-Aldrich (USA).

Instrumentation

Table 2 summarizes the used instruments.

Table 1. Textiles used

Textile	Composition [%]	Textile construction	Mass per unit area [g/m^2]	Supplier
CO white	100	twill 3/1	230	CHT R. Beitlich GmbH (Germany)
CO/PET orange	50/50	warp satin 4/1	340	Huntsman Textile Effects GmbH (Germany)
CO/PET camouflage	50/50	twill 2/1 core PET/shell CO	170	Bluecher GmbH (Germany)

Table 2. Instruments used

Instrument	Analytical method/method/remarks	Supplier
DSC Q20	differential scanning calorimetry (DSC), under 50 mL/min N_2, heating rate 10 K/min	TA Instruments (USA)
Bruker DMX300	NMR spectroscopy, ^{1}H, ^{13}C, ^{31}P	Bruker (USA)
SEM S-3400 N II	Scanning electron microscopy (SEM)	Hitachi High-Technologies Europe
X-Max 50 mm² SDD Detector	Energy disperse x-ray (EDX)	Oxford Instruments (UK)
HPV-E2, H emitter, Type 100 - 200	Ultraviolet A (UVA) print system lamp with dichroitic reflector for IR reduction, power 200 W/cm	Hoenle UV Technology (Germany)
linitester	Washing test	Atlas Material Testing Technology (Germany)
Nu-Martindale	Abrasion test	James H. Heal & Co. (UK)
Varian 720-ES spectrometer	Inductively coupled plasma optical emission spectra (ICP/OES)	Varian (Germany)
MarsXpress instrument	Microwave digestion	CEM (Germany)

Synthesis and characterization of allyl-oxy-polyphosphazene (PPZ)

Freshly sublimated hexachlorotriphosphazene (40 g), sulfamic acid (170 mg) and $CaSO_4$ x 2 H_2O (150 mg) were dissolved in 32 mL 1,2,4-trichlorobenzene under a nitrogen atmosphere and heated to 210 °C for 45-60 min. At the end of the reaction, a strong increase of the viscosity can be observed. The chloropolyphopshazene was precipitated by the addition of dry petroleum ether and the solids were washed twice with petroleum ether. The obtained polymer was dissolved in 100 mL THF. The concentration of the solution was determined by evaporating an aliquot and weighting of the residue. Afterwards, a freshly prepared sodium allyl alcoholate solution (4 eq. allyl alcohol with 1.25 eq. NaH in 50 ml THF) was added. The reaction mixture was rigorously stirred for 4 h at room temperature (RT), then refluxed for 6 h. The PPZ was precipitated by the addition of water. ^{1}H NMR (300 MHz, THF-d_8): δ 5.93 (ddt, J = 17.2, 10.4, 5.1 Hz, 1H), 5.29 (dd, J = 17.2, 1.8 Hz, 1H), 5.05 (dd, J = 10.4, 1.7 Hz, 1H), 4.48 (d, J = 5.5 Hz, 2H). ^{13}C{^{1}H} NMR (75 MHz, THF-d_8) δ 135.8, 116.0, 30.7. ^{31}P NMR (122 MHz, THF-d_8): δ –7.71. IR (ATR): 802 (P-O-C), 864, 923, 991, 1024 (P-N-backbone), 1101 (P-O-R), 1232 (P=N-backbone), 1423 (P-O-C), 1458 and 1647 (C=C), 2854 (C-H, sp^3), 2924 (C-H, sp^3), 3016 (C-H, sp^2), 3076 (C-H, sp^2) cm^{-1}. DSC (10 K/min, N_2 (50 mL/min)): T_G 180 °C, T_{Decomp} 282 °C.

Fabric UV treatment and characterization of the fixed PPZ

PPZ was dissolved in acetylacetone (25 wt%). The fabrics were wetted with 1 mL/g textile of the PPZ solution. The fabrics were irradiated single-sided for 10 min under an argon atmosphere. The distance between the light source and the sample was 20 cm. Subsequently, each sample was washed once in a textile linitester to remove non-bonded PPZ, afterwards dried at RT and weighed. In order to determine the phosphor content of the textiles quantitatively, 0.4 g were digested with 8.0 mL HNO_3 (65%) in a microwave digester at 180 °C. After digestion, the samples were diluted to 25 mL with water and measured by ICP-OES. The error of the phosphorus determination is less than 5%.

Washing resistance and abrasion test

In order to evaluate the washing fastness of the modified textiles, the materials were washed up to six times in a linitester according to EN ISO 105-C06 (liquor volume 150 ml, liquor ratio 1:80, ECE detergent 4.0 g/l, 30 min, 40 °C). The samples were then dried at room temperature and weighed. To investigate the fastness against mechanical stress, the modified textiles were subjected to 5,000, 10,000 or 50,000 abrasion cycles with a pressure of 9 kPa in a Martindale apparatus (abrasion test). Afterwards the samples were weighted. For the test an inverted Martindale setup has been used to get samples of at least 5 cm × 10 cm for a flammability test. The sample size was 140 mm diameter and the abrasive cloth (Martindale SM 25 (ISO 12947-1)) 40 mm diameter, with an abrasive exposed area of 110 mm diameter.

Evaluation of the flame retarding properties

All flame retardant and LOI measurements were carried out after at least one washing cycle. The flame retardant properties were measured according to DIN EN ISO 15025 (protective clothing - protection against heat and flame - method of test for limited flame spread), with a reduced sample size of 5 cm × 10 cm and a Proxxon lighter (combustion gas butane). In addition, selected samples were tested externally by Staatliches Pruefamt fuer das Textilgewerbe - University of Applied Science Hof (Germany) according to DIN EN ISO 4589-2 (limiting oxygen index, LOI, 0.5% steps), DIN 75200, DIN EN ISO 15025 and EN ISO 11925-2.

RESULTS AND DISCUSSION

Synthesis of allyl-oxy-polyphosphazene (PPZ)

PPZ was successfully synthesized by ring-opening polymerization of cyclic hexachlorotriphosphazene and subsequent nucleophilic substitution of the chlorine atoms by allyl alcoholate as shown in Fig. 1. The material is well soluble in acetylacetone.

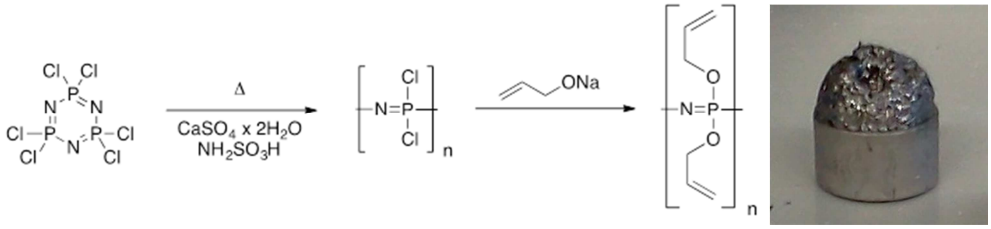

(a) (b)

Fig. 1. Allyl-oxy-polyphosphazene. (a) Synthesis, (b) after heating to 600 °C.

The ^{31}P NMR spectrum exhibits one singulett at -7.61 ppm, which indicates the presence of a non-crosslinked polymer with a typical chemical shift for a polyphosphazene. In addition, the ^{1}H NMR spectrum exhibits the typical signals for an allyl group. This correlates with the IR bands at 1232 cm^{-1} (P=N band) and at 1024 cm^{-1} (P-N band), which are characteristic bands for the polymeric backbone. The band at 1101 cm^{-1} represents the signal for the P-O-C ether. To achieve flame retardant properties, the flame retardant should have a decomposition temperature lower then the textile. Using DSC, we found a sharp exothermic degradation peak at 282 °C. When heating PPZ up to 600 °C the polymeric material shows an intumescent behavior. The foam-formation is shown in Fig. 1. In the case of fire the foam layer can act as a heat barrier.

Photochemical bonding of PPZ to textile materials

For our studies, we chose three different kinds of fabrics, one cotton fabric and two CO/PET blends (both 50/50 mixtures) used in common textile applications (e.g., clothing incl. protective clothing, car interior and furniture), where an improvement of the flame retardant properties is highly desired. The CO/PET blends differ in their fabric construction. The orange fabric is a warp satin woven material with one CO and one PET side. The second fabric (camouflage) consists of a PET core yarn with CO in the shell.

Beside phosphorus and nitrogen, which are responsible for the flame retardant properties of polyphosphazenes, our PPZ contains allyl groups, which are suitable for photo-induced grafting and cross-linking/homopolymerization. After wetting the textiles with a PPZ solution the materials were irradiated by a broadband-UV lamp under an argon atmosphere. Before characterization, the materials were washed once to remove non-bonded compounds. The PPZ-modified textiles were characterized by gravimetric measurements and SEM in combination with EDX for surface morphology and composition. Total phosphorus content was measured by ICP-OES after digestion. Table 3 summarizes the results. After the first washing step a high add-on of PPZ between 20 and 40 wt% was determined by gravimetry. An average weight loss after one washing step in the range of only 2–3% proofs the general efficiency of our photo-induced immobilization method. The phosphorus content found by ICP-OES is close to the calculated P content obtained by gravimetry. The surface P determined by EDX is between 18.5 and 22.5 wt%, which correlates with the mass fraction of P in the PPZ. Therefore, the layer thickness of immobilized PPZ must be higher than the information depth of the used EDX technology - thus at least 1.0 µm. The measured phosphorus contents (about 4 wt%) are higher than the recommended value for flame retardant properties (> 1.5 wt%).

Table 3. Summary of calculated and measured values for the P content of PPZ modified textiles

Textile	Add-on [wt%]	P calculated from add-on [wt%]	P measured[a] [wt%]	P surface[b] [wt%]
CO white	40.8	5.7	4.9	18.8
CO/PET orange	22.3	3.6	3.1	18.5
CO/PET camouflage	32.8	4.8	4.2	22.7

[a] Measured quantitatively by ICP-OES.
[b] Measured qualitatively by EDX.

Accordingly, flame retardant properties for the PPZ finished textiles can be expected. SEM micrographs (Fig. 2) show a film deposition of PPZ on the textile´s surface. As a consequence the corresponding ATR-FT-IR spectra of the textiles (Fig. 3) changes completely to the IR signals of pure PPZ; only the strong substrate signals like the carbonyl band of the PET part of the blends or the OH-signal of CO are weakly left. Taking the high add-on and the corresponding thickness of the

PPZ layer into account we assume that the PPZ is mainly bound by photo-induced homopolymerization between PPZ polymer chains yielding a stable film surrounding the fiber.

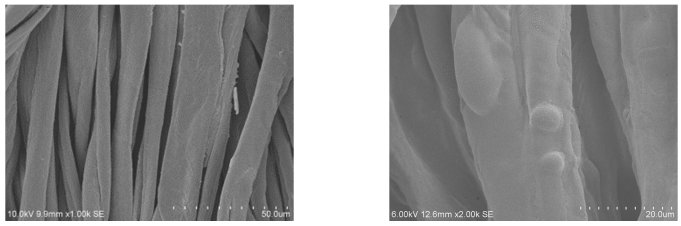

(a) (b)

Fig. 2. SEM micrographs of cotton fibers before (a) and after PPZ finishing (b).

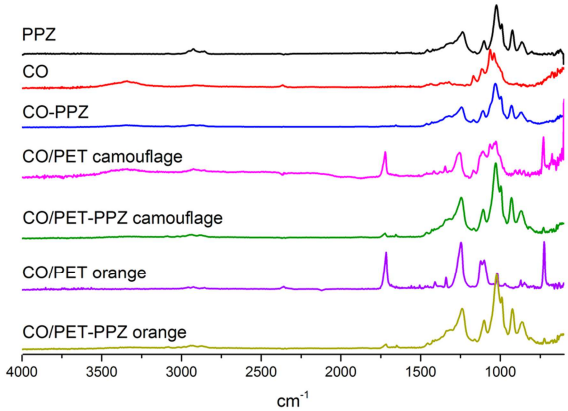

Fig. 3. ATR-IR-spectra of cotton/polyester blends and cotton fabrics before and after PPZ finishing in comparison to pure PPZ.

Flame retardant properties

In order to evaluate the flame retardant properties of the textiles, various methods were used. By measuring the limiting oxygen index (LOI) the minimum amount of oxygen in a mixture of oxygen and nitrogen is determined that is required to keep an ignited polymer burning. Normally, an increased LOI is accompanied by a lower ignitability and, therefore, improved flame retardant properties. For different textile applications different flammability testing standards exist. Here, we choose three methods. In the first test, the burning speed of a horizontal sample is measured, this test is described in DIN 75200 and is essential for textiles used in car interiors. DIN EN ISO 15025 represents a test for protective clothing. In addition, the test EN ISO 11925-2 was carried out to achieve the classification „normal flammability" according to DIN 4102-1 class B2 or EN ISO 13501-1 class E for building materials. Because of the vertical edge ignition applied in this test, the conditions are highly ambitious for textiles.

Table 4 summarizes the results of the various burning tests and the corresponding LOI measurements. Compared to the untreated materials, the LOI of the PPZ-finished textiles increases by 5-8%, which provides a first indication for a reduced flammability. During the horizontal burning test (DIN 75200), the untreated fabrics burn completely down with burn rates of 60-120 mm/min. In contrast, both modified CO/PET blends are self-extinguishing after the removal of the flame. In the case of modified CO, an acceleration of the burning was observed, however, the char yield is raised due to a significant carbonization of the material. By changing to a vertical flame test (DIN EN 15025), with a 10 s flame contact at the surface, the untreated materials burn down again

completely. In contrast, the PPZ-modified cotton and the CO/PET orange blend do not keep burning after the removal of the flame and no afterglowing was observed.

Table 4. Results of the LOI measurements and the standardized burning tests on PPZ-modified textiles

Textile	CO white	CO/PET orange	CO/PET camouflage
	LOI		
Untreated	17.5 - 18.0	18.5 - 19.0	16.5 - 17.0
PPZ	23.0 - 23.5	26.5 - 27.0	24.0 - 24.5
	DIN 75200		
Burning rate [mm/min]	142	0	0
Comment	carbonization	-	-
Test passed	no	yes	yes
Burning behavior of untreated material	burns down, 98 mm/min	burns down, 59 mm/min	burns down, 119 mm/min
	DIN EN ISO 15025		
Flame reaches upper or lateral edge	no	no	yes
Afterflame time [s]	0	0	20
Afterglow beyond flame area	no	no	no
Afterglow [s]	0	0	0
Appearance of particles	no	no	no
Burning particles	no	no	no
Hole formation	yes	no	no
Comment	-	-	extinguishes almost
Test passed	yes	yes	no
Burning behavior of untreated material	burns down within 8 s	burns down within 22 s	burns down within 11 s
	EN ISO 11925-2		
Reaching the test mark	7 s	5 s	4 s
Max. flame height	> 25 cm	> 25 cm	> 25 cm
Moment of max. flame height	12 s	12 s	10 s
Self-extinguished	0 s	0 s	5 s
Dripping	no	no	no
Test passed	no	no	no
burning behavior of untreated material	burns down, test mark 5 s	burns down, test mark 6 s	burns down, test mark 4 s

Finally, the three textile materials were subjected to a fire test with a 15 s vertical edge flame impingement test. All PPZ-modified textiles do not pass the test requirements, because the flame

reaches the upper test mark during impingement. However, a significant flame retardant behavior was observed. In contrast to the untreated materials, all PPZ-modified samples are self-extinguishing after the removal of the flame. Figure 4 illustrates the strong improvement of the flame retardant properties off PPZ-finished textiles compared to the blank substrates.

(a1) (a2) (b1) (b2) (c1) (c2)

Fig. 4. Blank (1) and PPZ-finished (2) textiles after the 15 s vertical flame test (EN ISO 11925-2). The test mark of 150 mm is visible as blue line on the fabric. (a) CO white, (b) CO/PET orange, (c) CO/PET camouflage.

Investigations on the permanence of the polyphosphazene finishing towards washing and abrasion

To evaluate the stability (fastness) of the PPZ modification, samples were subjected to several washing cycles and rigorous abrasive tests. Afterwards, the flame retarding properties were investigated according to the modified DIN EN ISO 15025 conditions. Figure 5 summarizes the add-on of the PPZ-layer on the orange CO/PET textile after different washing cycles. After the first washing cycle, non-covalently bonded PPZ was removed, which leads to a significant weight loss of nearly 3%. After the following washing cycles, no further weight loss was observed. Moreover, in all flame retardant tests, the specimens are self-extinguishing accompanied by a formation of a carbonized layer. Although the flame reaches the upper edge after six laundering cycles, a strong permanence of the flame retardant effect against washing can be assigned.

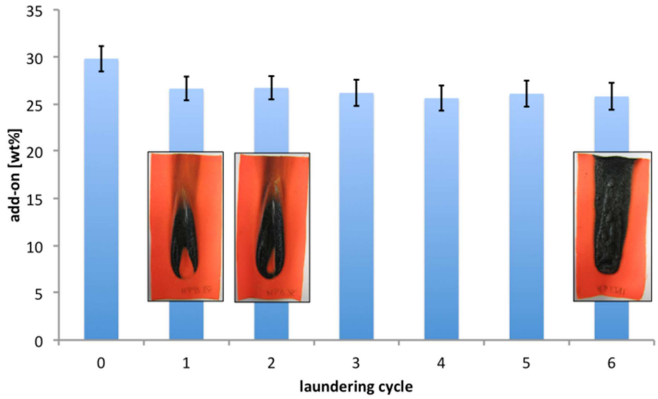

Fig. 5. Washing fastness of PPZ-modified CO/PET blend (PPZ-add-on and flammability behavior after six washing cycles).

In addition, the abrasion fastness of the PPZ-modified CO/PET (camouflage) blend was tested. After subjecting the textiles to 5,000, 10,000 or 50,000 abrasion cycles in a Martindale tester, the

flame retardant properties of the materials did not change significantly. All samples are self-extinguishing after the removal of the flame.

CONCLUSIONS

Polyphosphazenes belong to the class of inorganic polymers. Due to their phosphorus and nitrogen backbone, they exhibit excellent flame retardant properties. However, their industrial application in textile finishing was as yet limited by the lack of durable fixation strategies for a permanent flame retardant effect during the product´s lifetime. We succeeded in bonding a non-combustible and strongly foam-forming polyphosphazene derivative by an UV-induced grafting process to cotton and cotton/polyester blends in high add-ons up to 40 wt%. SEM imaging proofs the successful immobilization, and a total phosphorus content between 3-5 wt% was found. The polyphosphazene finishing leads to textiles with higher LOI. The textiles exhibit improved flame retardant properties and pass several standardized flammability tests such as standards for protective clothing and automotive textiles. The charred layer acts as a thermal isolating barrier layer and protects the underlying material. The permanence of the finishing was proven by washing and abrasion tests. The most essential results of PPZ-modified cotton and cotton/polyester blends are summarized in Table 5.

Table 5. Results of the LOI measurements and the standardized burning tests on PPZ-modified textiles (– = failed/no improvement, (+) = failed, but significant flame retardant effect, + = passed/strong improvement)

Test	CO white[a]	CO/PET orange[a]	CO/PET camouflage[a]
LOI[b]	+	+	+
DIN 75200	-	+	+
DIN EN ISO 15025	+	+	(+)
EN ISO 11925-2	(+)	(+)	(+)
Washing fastness[c]	+	+	+
Abrasion fastness[c]	+	+	+

[a] – = failed/no improvement, (+) = failed, but significant flame retardant effect, + = passed/strong improvement.
[b]after one laundering cycle
[c]modified DIN EN ISO 15025 procedure.

In consideration of these excellent results, we state that functional polyphosphazenes could be a new class of permanent and halogen-free flame retardant agents for textile applications in the near future. However, competitive and commercial products for the textile industry have to be water-based (water-soluble or at least water-dispersible). Therefore, a future focus will be the synthesis of innovative polyphosphazenes, which combine functional side groups for a permanent attachment and hydrophilic side groups for an improved solubility in aqueous systems.

ACKNOWLEDGEMENT

The authors wish to acknowledge financial support by the Forschungskuratorium Textil e.V. for the project IGF 16780 N. The support was granted within the program Industrielle Gemeinschaftsforschung (IGF) from resources of the Bundesministerium für Wirtschaft und Energie (BMWi) via a supplementary contribution by the Arbeitsgemeinschaft Industrieller